Available online www.jsaer.com

***Journal of Scientific and Engineering Research*, 2022, 9(11):209-226**

Research Article

ISSN: 2394-2630
CODEN(USA): JSERBR

A Holistic Framework for Estimation of Aggregate Inventory for Road Construction Using Google Earth Pro®: A Case Study of Libya State

Nassraddin A. Ibrahim[*,1], Gabriel J. Assaf[1] and Yannic Ethier[1]

[1]Laboratory for Geotechnical and Geoenvironmental Engineering (LG2), École de technologie supérieure, 1100 Notre-Dame Ouest, Montreal, Quebec, H3C 1K3, Canada
*Correspondence: nassraddin.ibrahim.1@ens.etsmtl.ca; Tel.: +1 5147707010

Abstract In terms of non-fuel minerals, natural aggregates are the world's most valuable and are the third most consumed resource worldwide after water and air. Despite the availability of materials, transportation agencies design their roads according to traffic levels and soil conditions. In many cases, a national inventory is not carried out thoroughly. Therefore, a preliminary estimate of a quarry's capacity for a road project generally will not be available or accurate until after the contract has been awarded. It is estimated that thousands of kilometers of roads will need to be constructed in the developing world in the coming decades in order for many economies to develop. In order to optimize the use of quality aggregates, it is important to identify and catalog all existing road construction materials in those countries by performing an inventory of available source materials such as sand and gravel. In this study, Google Earth Pro® software is used to estimate a potential aggregate inventory using national data publications on a case study of Libya. Based on the study results, there are 38.3 million tons of aggregates available for road construction from 21 active quarries. To sum up, sustainable road design would greatly benefit from this information, helping to reduce aggregates, costs, time, and air pollution.

Keywords Materials, Google Earth Pro®, Satellite imagery, Quarry, Inventory, Sustainability, Estimation

Introduction

The vast majority of infrastructure sectors today acknowledge sustainable development in some form, thereby managing it in some way. Hence, the main sustainable sector of infrastructure is roads. A society's development is dependent on the construction of roads. It relies heavily on mined and quarried raw materials, such as sand and gravel (aggregates) [1, 2, 3, 4, 5, 6]. After air and water, natural aggregates are the third most consumed resource in the world, and they are the most valuable mineral commodity in the world [7, 8, 9, 10]. A significant part of the sustainable use of mineral aggregate resources is the identification of potential sites for aggregate quarries [11; 12; 13, 14, 15, 16].

A study by Wu et al., [17] indicated that mapping and exploring large unknown wild environments takes a lot of time. Information about the location of roads can be obtained from satellite images. A method of topological road network construction using Google Earth Pro® was proposed in this paper. The paths plotted on topological maps can be used as a basis for local planning. The topological road network can be constructed accurately with Google Earth Pro® based on real-time vehicle experiments. In the wild, unknown environment of a topological map, vehicles can follow the directions provided by the map to reach their destination quickly. In addition, as noted by Derrow-Pinion et al., [18], travel-time predictions are of significant importance in transportation networks because web mapping services such as Google Maps serve huge amounts of travel-time queries from both individuals and businesses. Additionally, this task requires a thorough understanding of complex

spatiotemporal interactions (spatial modeling of the topological properties of a road network as well as anticipating future events like rush hours). Thus, it is an ideal target for learning graph representations at scale. Google Maps has deployed an estimator of estimated time of arrival (ETA) using a graph neural network. The main architecture of our model consists of standard GNN building blocks, as well as ration-resistant and production-ready training schedule methods like Meta Gradients. Providing prescriptive studies of various architectural decisions and training regimes as well as qualitative analyses of real-world situations in which our model excels. With our GNN deployed, negative ETA outcomes were significantly reduced in several regions compared to the previous production baseline.

Furthermore, in developing countries, it may be difficult to gather relevant information about road construction materials. Utilizing general geological information from Google Earth and satellite imagery may lead to the discovery of potential sources of materials. A popular free virtual globe application, Google Earth provides a wealth of images taken around the globe, which have been widely used in a wide range of industries [19; 20; 21, 22, 23].

Likewise, there have been studies that have used Google Earth in order to determine the distribution of quarries, the outline of quarries, and the borders of quarries [24; 25; 26, 27]. A key feature of Google Earth is its ability to access mines and quarries directly from freely available data sets, eliminating the need for site visits. As far as cost and time are concerned, that is a very efficient method. The quantity of the RAP inventory was estimated using Google Earth by [28; 29; 30]. Additionally, it can be used to map roads and geographical features, calculate the size of a quarry, and demarcate its boundaries [31; 32; 33, 34, 35]. It is possible to better plan the exploitation of aggregate quarries for transportation infrastructure with this information.

Moreover, the Libyan government uses 21 quarries as a source of aggregate for road construction. Based on their geographical distribution, the main quarry locations can be divided into four main regions. The Northwest region has six quarries, the Central region has five, the Northeast region has five, and the Southwest region has five (Idris, 2012). According to this paper, the quarry sites in Libya were located, the area was calculated, and potential aggregate materials stockpiles were estimated using Google Earth Pro®. Likewise, conducting feasibility studies and budget management and allocation of funds for any project requires an early estimate of the construction cost. Road costs vary depending on the number of users, the area, the quality, and the construction and structural system [36]. In ancient times, karez were used for large-scale irrigation and water conservation in the arid regions of Central Asia. Turpan, which is located in the Xinjiang Uyghur Autonomous Region, has the most extensive and concentrated distribution of karez shafts in China. There are tens of thousands of shafts, some of which are in use and are living cultural heritage. According to radiocarbon (14C) dating, some karezs are over 600 years old. It is important to study karez geology, hydrology, oasis, climate change, and development history in Turpan. With the development of the population, arable land, industrialization, and urbanization, karez systems are facing the risk of abandonment. Detailed karez distribution mapping or dynamic monitoring data are important for their management or analysis; although there are related methods, due to Turpan's large desert and "Gobi" environments, field surveys are time- and energy-consuming, and some areas are difficult to access. Precise shaft locations and distribution maps are scarce and often lack georeferencing. The distribution and preservation of karez have not yet been fully explored. In this study, we evaluated the effectiveness of You Only Look Once version 5 (YOLOv5) in automatically detecting karez in high-resolution images of the Turpan region. The proposed model was a post-processing step to reduce the false karez identified by YOLOv5. The results demonstrate that YOLOv5 and post-processing techniques can be used to detect karez automatically. The detected results demonstrate that karez is linearly aligned. Target detection based on YOLOv5 and post-processing can greatly improve automatic shaft identification and is therefore useful for the fine mapping of karez. We also applied this method in Shanshan County (for which no detailed mapping data on karez had been obtained before) and successfully detected some karez that had not been archived before. The number of shafts in Turpan is 82,493. Through DBSCAN clustering, it was identified which karez line belonged to which shaft; the number of sections of karez that have been used is 5057, which have a total length of 2387.2 km. The karez line obtained was overlaid with the crop-land data, and the positional relationship between the karez line and the crop land was analyzed. The cultivated area is mainly surrounded by karez. The proposed method can potentially be applied to construct of inventory of all karez shafts globally.

Li et al., [37] evaluated the effectiveness of You Only Look Once version 5 (YOLOv5) in detecting karez in Turpan region images at high resolution. In order to reduce the number of false karez detected by YOLOv5, a

post-processing step was proposed. The detected results are sufficient to capture the linear alignment of karez when using YOLOv5 and post-processing techniques. Automatic shaft identification can be greatly improved by using YOLOv5 and post-processing, so it is useful when mapping karez finely. This method was also applied in Shanshan County (where no detailed mapping data on karez had previously been obtained) and some previously unarchived karez were detected. With 82,493 shafts, Turpan has the most shafts in the world. As a result of DBSCAN clustering, it has been identified which karez lines belong to which shaft; a total of 5057 karez sections have been used, which total 2387.2 km in length. The karez line obtained was overlaid with the crop-land data, and the positional relationship was examined. It is basically surrounded by karez around the cultivated area. Using the proposed method, an inventory of all karez shafts worldwide can be constructed. According to Li & Lu [38], fragmented datasets are better at displaying the site environment cognitively. In Google Earth, the proposed framework integrates unordered images, geometric models and the surrounding environment through Keyhole Markup Language (KML). It was proposed that unsequential aerial images and ground images can be geo-referenced without using ground control in order to place them into the physical coordinate system of Google Earth. A KML and cloud storage-based data management system is conceptualized to conglomerate geometric models, site images, and panoramic images with the surrounding environment in 3D GIS. Using information management, integration, and visualization, the research delivered construction engineers with a low-cost and low-technology solution for representing a dynamic construction site.

Literature Review

Ashtiani et al., [28] claimed that reclaimed asphalt pavement (RAP) contributes about 20% of aggregate production nationwide by weight, making it the most recycled material. The purpose of this study was to describe an economical method of estimating the volume and weight of RAP stockpiles using Google Earth Pro® software and publicly available information. The study examined Washington State as a case study. In addition, it is possible to aggregate this information over an entire region or state and within a range of years to provide accurate RAP locations. Thus, the findings in this study differ from those based on receipt/use survey data from the National Asphalt Pavement Association (NAPA) for Washington State over the past decade. In addition to discussing data reliability, inconsistencies with NAPA results, and alternative approaches to utilizing RAP oversupply, there will also be a discussion of alternative approaches to utilizing RAP. According to Ashtiani & Muench [39], effective sustainability management is hampered by the lack of data-driven benchmarks with which to measure best practices in the $100 billion road construction industry. Among the 12 metrics introduced in the first sector were water use, vegetated areas, stormwater runoff treatment, lighting power, construction waste generation, local material use, pedestrian areas and bicycle facilities, recycled content, pavement reuse, greenhouse gas emissions, and energy consumption during construction. Benchmarks for sustainable performance were established using data from 33 projects to provide quantitative measures for the performance metrics introduced in this study. Additionally, a life cycle assessment of these projects found that paving materials contributed most to greenhouse gas emissions and energy consumption. Therefore, it wasn't possible to incorporate all items into the analysis. In addition, greenhouse gas emissions and energy consumption can also be predicted based on project prices alone.

Furthermore, in Ontario municipalities, Simth [40] reported that asphalt is used for more than 6.5 million tonnes of construction and maintenance of municipal roads annually. In the construction of roads, reclaimed asphalt pavement (RAP) has been proven to provide sustainable structures without compromising materials integrity. The use of RAP in asphalt pavement mix designs is currently allowed by less than two-thirds of the municipalities in Ontario, and most of them implement it only in base courses. Using such sustainable infrastructure approaches would result in cost-effective infrastructure spending, preserving virgin materials resources, as well as limiting greenhouse gas emissions by reducing asphalt consumption and utilizing locally available recycled materials. The purpose of this paper was to quantify the current availability of RAP in the province of Ontario, as well as provide information on trends in its consumption. To obtain a database of RAP stockpile locations throughout Ontario, an environmental scan was conducted. With the help of Google Earth Pro® software, volume measurements were conducted. A further calculation was carried out to estimate the weight of the RAP inventory as well as the trend in its consumption. In this way, this study could contribute to more sustainable material use in infrastructure. Moreover, it was pointed out by Cass and Mukherjee [41] that obtaining materials for highway infrastructure construction, maintenance, and rehabilitation emits large amounts

of greenhouse gases (GHGs). The purpose of this paper was to develop and illustrate a method for state agencies to use to quantify the life-cycle emissions associated with pavement designs. Life cycle assessment (LCA) integrates process-level construction data into existing LCA methods. A method was developed that can be applied to develop and analyze life-cycle inventories for the construction phase of the project. During construction and rehabilitation operations, it describes collecting data on material and equipment usage on-site. In contrast to traditional approaches comparing alternative pavement materials or designs based on estimated inventories, this paper proposes that a context-sensitive process-based approach be used to calculate greenhouse gas emissions using a hybrid life cycle assessment that utilizes actual construction data. Also, a concrete pavement rehabilitation case study was performed to illustrate the proposed method. Based on the findings, total CO_2 emissions for Hybrid Models 1 and 2 were 787.19 tons and 1,383.28 tons per lane mile, respectively; 90% and 94% of the total CO_2 emissions during the construction phase for Hybrid Models 1 and 2 are attributed to the production of materials, equipment, and fuel used to construct the project; equipment use and transportation impacts together account for only 6-10% of total emissions.

Choi et al., [42] examined the size effect on shear failure of deep concrete beams with Basalt Fiber Reinforced Polymer (BFRP) bars. A mesoscale numerical model for the deep concrete beam with BFRP bars was built to explicitly model the shear failure, considering concrete heterogeneity and concrete/bars interaction. The mesoscale simulation approach was firstly verified against the available test observations. It was then utilized to study the shear failure of geometrical-similar concrete deep beams having different structural sizes with BFRP bars and steel bars. The influence of beam depth, stirrup ratio and reinforcement type (i.e., steel bars and BFRP bars) on the shear failure and the corresponding size effect of concrete deep beams was explored. The simulation results indicate that: 1) the failure modes of concrete deep beams with BFRP bars and steel bars are basically similar, and they all exhibit noticeable size effect; 2) stirrups (i.e., steel bars and BFRP bars) can hinder the development of diagonal cracks within concrete, and thus weaken the size effect in shear strength; 3) the shear failure in beams with BFRP bars presents more substantial size effect than that of beams with steel bars; 4) the calculation models of shear capacity in the international codes do not apply to concrete deep beams with BFRP bars. Moreover, it is found that the size effect law developed previously can also be suitable for the shear failure of concrete deep beams with BFRP bars. Furthermore, Ning et al., [43] used of fiber-reinforced polymer (FRP) rebars in lieu of steel rebars has led to some deviations in the shear behavior of concrete members. Several methods have been proposed to forecast the shear capacity of such members. Nonetheless, there are differences in the methods of considering the various parameters affecting shear capacity, and some of them provide widely scattered and conservative results. This paper presents a hybrid of the Bayesian optimization algorithm (BOA) and support vector regression (SVR) as a novel modeling tool for the prediction of the shear capacity of FRP-reinforced members with no stirrups. For this purpose, a large dataset of simply supported beams and unidirectional slabs reinforced with FRP were utilized. The model performance was assessed using several statistical performance indicators and compared with the Japan Society of Civil Engineers (JSCE), British Institution of Structural Engineers (BISE), Canadian Standard Association (CSA), and American Concrete Institute (ACI) design codes and guidelines, as well as some other artificial intelligence (AI) models. For development of the model, all the hyperparameters, i.e., kernel function type, epsilon, box constraint, and kernel scale, were optimized using the BOA technique. The k-fold cross validation approach was utilized to avoid overfitting of the model. It was found that the mean, median, standard deviation, minimum, maximum, and interquartile range of the developed hybrid model predictions are very close to the experimental results. The predicted results overlap the experimental data with a coefficient of determination of 95.5%. The plot of relative deviations and residual plots are scattered around the zero reference line with low deviation, which indicates that the model is reliable and valid. The error terms (e.g., mean absolute error, root mean square error) obtained for all specimens were 4.85 and 11.03, which are very low values. The correlation coefficient (R) and fractional bias (FB) were found to be 0.977 and 0.0033, which are very close to 1 and 0, respectively, thus implying a reliable prediction. The comparative investigations with other codes and guidelines show that the hybrid BOA–SVR model predictions are more accurate and robust than those of the other models.

Ning et al., [43] stated that the use of street view imagery such as Google Street View is widespread in everyday life. The detection and mapping of objects such as traffic signs and sidewalks has been studied for many years in urban built-up environments. The use of automatic vertical measurements in large areas is underutilized in those studies even though mapping in the horizontal dimension is common. A variety of studies can benefit from the horizontal information provided by street view imagery. A noteworthy application is estimating the lowest floor

elevation, which is crucial for assessing flood vulnerability and calculating insurance premiums. The purpose of this article was to investigate vertical measurement in street view imagery using the principle of tacheometric surveying. As part of the case study of low floor elevation estimation using Google Street View images, we trained a neural network (YOLO-v5) for door detection and measured the height of the door using the fixed height of the door. Based on the results, the average error of the estimated elevation is 0.218 m. To determine the height from the roadway surface to the target, Google Street View depth maps were examined. An automated elevation estimation pipeline based on street view imagery was proposed, and it was expected to benefit future terrain-related studies. The authors of Yang et al., [44] noted that rural areas in China have a large population. Rural households typically discharge sewage without much treatment throughout the country. In order to study the impacts of rural households on their surroundings, it is essential to understand rural population distribution. The availability of high-resolution spatial datasets on rural population distribution in China is limited. Using images from Google Earth, this study constructed a high-resolution map of rural population distribution in eastern China from a town's image from Google Earth. Results of the study demonstrate that texture analysis in combination with other processing procedures can be used to extract man-made building features from the image, which in turn can be used to map the distribution of rural populations. The development of spatial datasets on rural population distribution in many parts of the world may be possible through this approach. As reported by Lee et al., [45], the Land Transport Authority (LTA) of Singapore uses the geometric design standard for road markings published in the "Standard Details of Road Elements" (SDRE) of Singapore to estimate the distance between road features, particularly useful when performing speed analyses. The SDRE was compared with onsite measurements (by measuring tape, total station, or 3D laser scanner) taken at various locations in Singapore, as well as distance estimates using Google Earth Pro®. According to the results presented here, the SDRE accurately estimated 85.7% of all corresponding onsite measurements to within 5%, and it can be relied upon to reconstruct crashes. The distance accuracy of the geometric design standard (SDRE) and Google Earth Pro® was also evaluated in this study, and it was found that both methods were robust and accurate, with an overall average absolute percentage error less than 1%, making them ideal for obtaining measurements in crash reconstruction, especially when the site of interest is inaccessible. Google Earth Engine (GEE) was used by Lin et al., [46] to analyze land cover classification and the spatial pattern of major land cover changes on Haitan Island, China, from 1990 to 2019. Landsat images based on the random forest supervised algorithm were transformed into tasseled caps and analyzed with multiple spectral bands (RGB, NIR, SWIR), vegetation indices (NDVI, NDBI, MNDWI), and tasseled cap transformations. Overlay processes (transfers from and to) between 1990 and 2019 were analyzed, and the accuracy ranged from 88.43% to 91.08%, while Kappa coefficients ranged from 0.86 to 0.90. Other land, cultivated land, sandy land, and water area decreased from 1990 to 2019, while forest and built-up land increased. As a result of reforestation, cultivated land reduction, and built-up land expansion, the land cover of Haitan Island has changed dramatically. On Haitan Island, forests, cultivated lands, and built-up lands have changed mainly due to a 'Grain for Green Project' and a 'Comprehensive Pilot Zone' policy. Reforestation, population growth, and economic development were the major drivers of land use change. As a result of this study, continuous monitoring of the impact of reforestation efforts and urbanization on an island environment was demonstrated for the first time.

Methodology

Studies like in many developing countries, there is no available up-to-date aggregates resources information in Libya due to the many challenges the country has faced. Google Earth Pro, in conjunction with available data from the best available national data publications from reliable scientific journals and sources, unpublished works from Libyan universities, and from direct contact with people working in the Ministry of Communications and Transport and the Roads and Bridges Authority. Google Earth Pro was used to estimate potential aggregate materials quantities in Libya. Work followed these Four basic steps as shown in Figure 1: 1) Locate quarries sites, 2) identify quarries' potential aggregates, 3) estimate the volume and quantity available of aggregates. 4) estimate the distances of quarry locations from the closest main road. Figure 2 illustrated the material quantity volume measurement procedure. Because the extraction activities of the quarries are continuous. This method should be repeatable every few years to measure and track the change in the inventory. so long as adequate, Google Earth high-resolution aerial images are available.

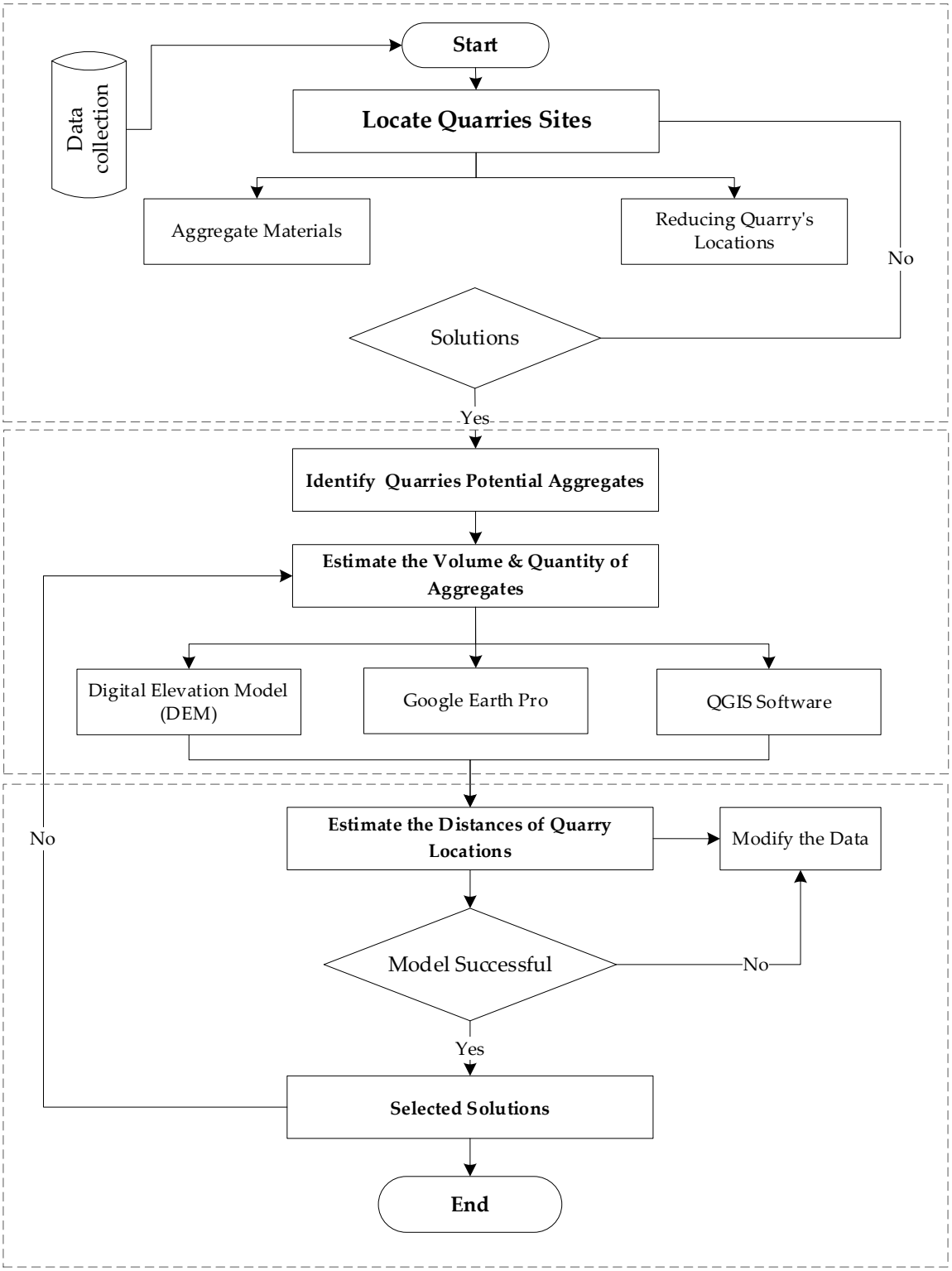

Figure 1: Research framework

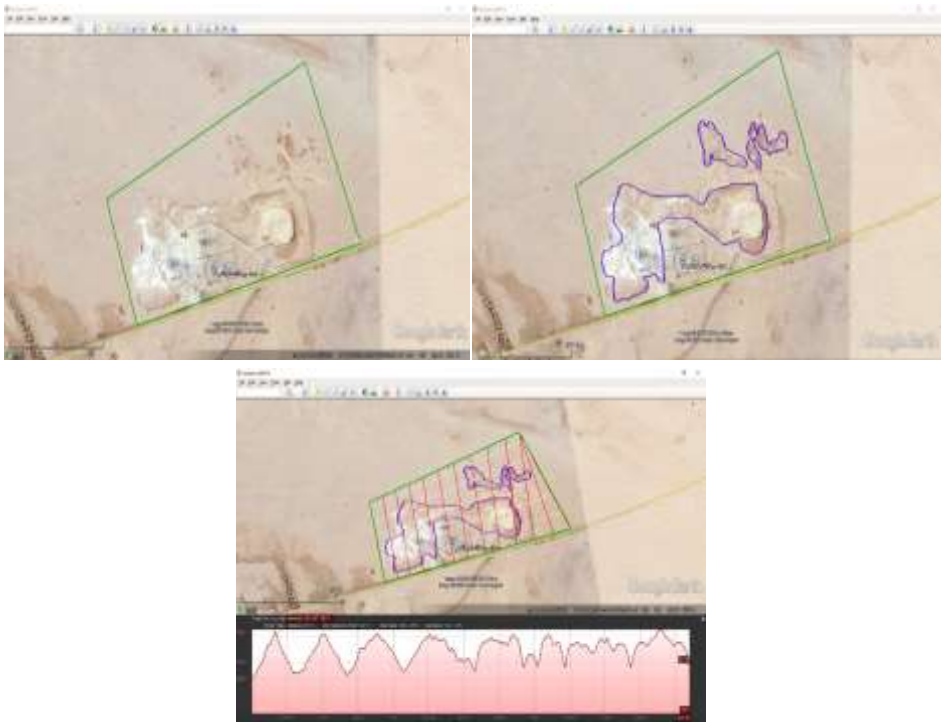

Figure 2: The material quantity volume measurement procedure: A) the polygon for the area of the quarry, B) the extraction operation area of the quarry blueline, C) a cross-section and elevation profile using Google Earth 3D model.

Step1: Locate quarries sites

Quarries usually are preferred to be located near road projects. Due to the following reasons: 1) Aggregate materials have low-value commodities. Therefore, the transporting of the aggregate for a long distance to the operation location can considerably increase the price of the aggregate. 2) Reducing the costs for the construction and maintenance of the roads to the quarries. Aggregates quarry's locations were initially located using data was collected from the best available national data publications from reliable scientific journals and sources, unpublished works from Libyan universities, and from direct contact with people working in the Ministry of Communications and Transport and the Roads and Bridges Authority. The most recent information was used to determine the locations available. A total of 21 potential aggregates quarries locations divided into four main regions according to their geographic division were detected.

Step 2: Identify quarries' potential aggregates

Google Earth satellite images were used to scan quarry locations and their surrounding areas to determine the quarry's borders and aggregate inventory. The Quarry border was identified by the excavation and rock extraction activities in the area. However, sometimes the quarry's borders and aggregate inventory were sometimes difficult to identify because of the poor quality of the satellite images in some areas. The locations of the determined quarries were pinned and organized in Google Earth Pro.

Step 3: Estimate the volume and quantity available of aggregates

To estimate the potential quantities of aggregates, Google Earth Pro used to measure the base area. Area sketching and cross-sectioning are the best methods to determine the average area and depth, In Google Earth pro, from the satellite image, the polygon feature can create a cross-sectional and measuring of any area. Elevation profiles can be extracted from Google Earth Pro from any linear path on the earth's surface. Fig 3-c

shows an example of a cross-section line in red and the elevation profile. using this to provide the average profile height. Thus, the linear path across the quarry can determine the average height difference between the bottom and the top of an unextracted area of the quarry which represents the height of the remaining material inside the quarry. Therefore, for every quarry location, a polygon shape was drawn for the area measurement of potential materials so that a simple volume calculation can determine the quantity available. In addition, the Digital elevation model (DEM) was created to validate the effective heights of the aggregates in the quarry. In comparison with the in-situ surveying methods, Google Earth Pro can provide statistically reliable elevation data [47]. Therefore, elevation data from Google Earth pro were imported into QGIS software to create the DEM illustrated in Figure 3.

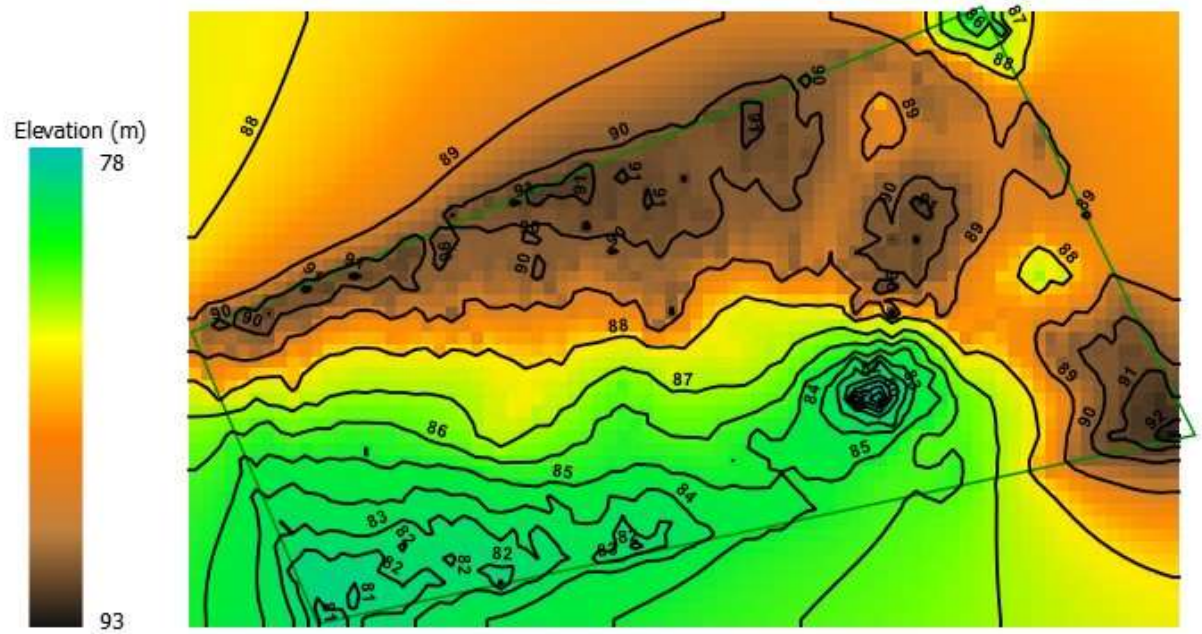

Figure 3: Digital elevation model (DEM) of the heights of the aggregates in the quarry.

The quantities in tons are calculated by multiplying the volume of the deposit by the density factor.

Tonnage = Area x Thickness x Density Factor.

This factor is approximately the number of tons in a 1-meter thick bed of gravel and sand, an area of 1 ha, assuming an average density of 1770 kg/m3 for sand and gravel and 2649 kg/m3 for lime stone. Tonnage calculated in this manner must only be considered as an estimate [48].

Step 4: Estimate the distances of quarry locations from the closest main road

The locations of the determined quarries were pinned and organized in Google Earth Pro. To estimate the distances between the quarries to the main roads Google Earth Pro offers a feature (add path), to measure the length of a path and distance between locations directly from the satellite images. Therefore, by identifying the locations of quarries and drawing paths to the closest main road, can be calculated and estimated approximate distances between them. The shortest distance to the road network indicates the suitability of a quarry's location as an aggregate resource.

Overall, estimates of overall aggregate inventory are most likely to be affected by the following sources of error: imprecise outline borders of the quarry and imprecise effective heights due to low-resolution images in some areas, and imprecise density assumptions. The Quarry border was identified with the excavation and rock extraction activities in the area. For the actual height, the assumption uses a mean of the estimated value and an average of 1770 kg/m^3 and 2649 kg/m^3 for density depending on rock type.

Model Implementation

This study's database contains the following information on all quarries: the location and topography of the quarries, measured base area, rock types and calculated inventory, and the distances of quarry locations from the closest road.

The Sources and Quantities of Potential Aggregate Resources

The potential sources of materials are likely to be found based on general geological information, e.g. from Google Earth and satellite imagery. However, the available resources for gathering relevant information on road construction materials may be limited in many developing countries. Furthermore, the detailed exploration fieldwork and extensive geotechnical tests of appropriate geological formations are mandatory to determine potential aggregate areas. Aggregate resources occur naturally and are fixed in location, so they must be extracted from where they are found. However, is not easy to be extracted from any location. There are a variety of geological variables that affect their location, including resource quality and quantity, depth of overburden, and other factors. In Libya, the main quarry locations divided into four main regions according to its geographic division, Northwest, Central, Northeast and the Southwestern region as shown in Figures 4 and 5. Each region has a certain number of quarries were identified at the level of Libya used as a source of aggregate for road construction [49]. In Libya, there are 21 quarries, six quarries located in Northwest, five quarries located in the Central region, five quarries located in the Northeast, and five quarries located in the Southwest region. Table 1 illustrates the number and location of the quarries in each region.

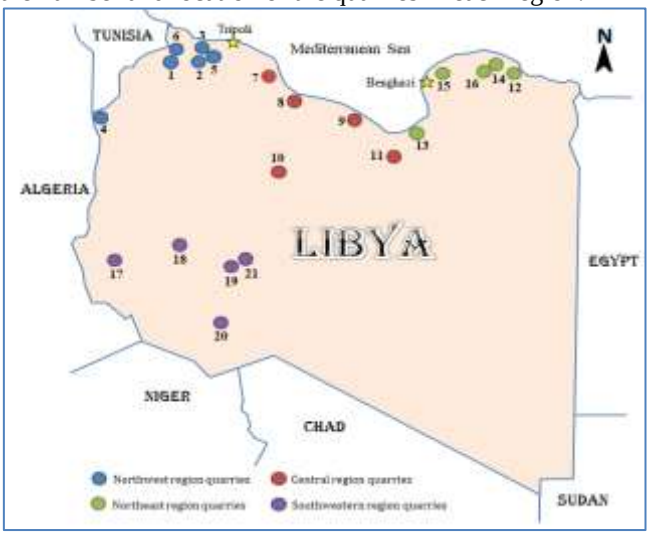

Figure 4: Quarry locations [49].

Figure 5: Locations of quarries on Google maps.

Table 1: Number and location of the quarries in each region.

No	Quarry name	Location	Topography
		Northwest Region	
1	Al Enetak	Qasar Al haj	Hilly
2	Alkalej	Al Rabta	Hilly
3	Al hani / Strabagh	Ras Allafah	Hilly
4	Vyadoket Croatian	Gadamis	Hilly
5	Saraya	Ras Ghdah	Mountainous
6	Alasdeka	Al jawsh	Hilly
		Central Region	
7	Cyprus G & P	Al-Hesha - Sirte	Hilly
8	Juba Contracting	Sirte 50 Km	Hilly
9	Yoksel Brogi Quarry	Bin Jawad	Hilly
10	Public Works Authority Quarry	Sawknah- Al Jafrah	Mountainous
11	Ostai Quarry	Maradah	Mountainous
		Northeast Region	
12	Yuksel, Turkish Quarry	At Tamimi	Hilly
13	Yuksel Quarry	Al Brega	Hilly
14	Arab Group Contracting Quarry	Mechili Al Rmelat	Hilly
15	Al Hani Quarry	Al abyar	Hilly
16	Mappa Turkish Quarry	Mechili	Hilly
		Southwest Region	
17	Ubari Quarry	Alawenat	Hilly
18	Turkish Mitch Quarry	Ubari	Hilly
19	Victoria Quarry	Umm Al Aranib	Hilly
20	Al Amal Tareq Quarry	Qatrun- Tagerhi	Hilly
21	Al-Saraj Quarry	Al Bedar	Hilly

Northwest Region

Six quarries of sand and gravel are available as potential sources of aggregates. Al Enetak Quarry, Alkalej Quarry, Al Hani / Strabagh Quarry, Vyadoket Croatian Quarry, Saraya Quarry and Alasdeka Quarry. These quarries cover the area from the city of Tripoli to the city of Ghadams, along with the al Jabal al Gharbi Mountain in the Northwest region. All quarries are natural valley deposits except the Saraya Quarry is a bedrock aggregate. These quarries have about a total area of 98.9 ha with possible resources approximately 12 million tons of aggregate material is still available for extraction. The highest potential amount of aggregates is 3.5 million tons in the Saraya Quarry and the lowest potential amount is 0.4 million tons in Alkalej

Table 2: Number and location of the quarries in each region.

Region	No	Location	Quarry	Rock types	Potential reserve area (Hectares)	Possible Aggregate Resources (Million Tonnes)
Northwest	1	Qasar Al haj	Al Enetak	Dolomite	18.3	2.1
	2	al Rabta	Alkalej	Dolomite	7.9	0.4
	3	Ras Allafah	Al hani / Strabagh	Limestone	14.8	1.7
	4	Gadamis	Vyadoket Croatian	Limestone	17.3	2.0
	5	Ras Ghdah	Saraya	Dolomite	20.2	3.5
	6	Al jawsh	Alasdeka	Dolomite	20.4	2.3
Central	7	Al-Hesha- Sirte	Cyprus G & P	Limestone	17.7	1.1
	8	Sirte 50 Km	Juba Contracting	Limestone	23.5	2.1
	9	Bin Jawad	Yoksel Brogi	Limestone	32.4	2.9
	10	Sawknah-Jafrah	Public WorksAuthority	Limestone/ Dolomite	14.5	2.3
	11	Maradah	Ostai	Limestone	17.4	2.8
Northeast	12	At Tamimi	Yuksel, Turkish	Limestone	33.4	3.5
	13	Al Brega	Yuksel	Limestone	28.1	2.0
	14	Mechili- Rmelat	Arab Contracting Group	Limestone	29.7	1.6
	15	Al abyar	Al Hani	Limestone	26.7	2.4
	16	Mechili	Mappa Turkish	Limestone	14.5	0.8
Southwest	17	Alawenat	Ubari	Sand stone	10.5	0.6
	18	Ubari	Turkish Mitch	Sand stone	20.1	1.4
	19	Umm Al Aranib	Victoria	Sand stone	16.2	0.9
	20	Qatrun- Tagerhi	Al Amal Tareq	Sand stone	18.9	1.0
	21	Al Bedar	Al-Saraj	Sand stone	12.6	0.7

Central Region

The central region extended from Misrata to Bin Jawadi covering the Gulf of Sirt is predominated by saltmarsh, and lagoons. Five quarries have been identified by ministry of transportation for sand and gravel as potential sources of aggregates. Cyprus G & P quarry, Juba Contracting Company quarry, Yoksel Brogi company Quarry, Public Works Authority Quarry, and Ostai company quarry. Two of these quarries are bedrock aggregate which is Public Works Authority Quarry and Ostai Quarry the other is natural valley deposits. The highest potential amount of aggregates is 2.9 million tons in the Yoksel Brogi Quarry and the lowest potential amount is 1.1 million tons in Cyprus G & P Quarry. However, the quarries in the region have a total area about 105.5 ha with possible resources approximately 11.1 million tons of aggregate material is still available for extraction.

Northeast Region

This area extended from the Al Brega plane and rises gradually to the East, to the sedimentary rocks of Jabal Al Akhdar to Tobruk city in the border between Libya and Egypt in the east. Five selected quarries of sand and gravel have been chosen as potential sources of aggregates: Yuksel, Turkish Quarry, Yuksel Quarry, Arab Group Contracting Quarry, Al Hani Quarry, and Mappa Turkish Quarry. All these quarries are natural valley deposits. These quarries cover an area of about 132.4 ha with possible resources approximately 10.2 million tons of aggregate material is still available for extraction. The highest potential amount of aggregates is 3.5 million tons in the Yuksel, Turkish Quarry and the lowest potential amount is 0.8 million tons in Mappa Turkish Quarry.

Southwest Region

The southern and hyper-arid central inland of Libya is covered by gravel plains, Mesozoic limestone, and sandstone plateau. The Quaternary sand dunes cover most of the interior regions, such as Sirte Basin. Five quarries have been selected of sand and gravel as potential sources of aggregates: Ubari Quarry, Turkish Mitch Quarry, Victoria Quarry, Al Amal Tareq Quarry, and Al-Saraj Quarry. All these quarries are natural valley deposits. These quarries have a total area of about 78 ha with possible resources approximately 5 million tons of aggregate material is still available for extraction. The lowest potential amount is 0.6 million tons in Ubari Quarry, however, the highest potential amount of aggregates is 1.4 million tons in the Turkish Mitch Quarry.

The Distances of Quarry Locations from the closest Road

Aggregate is materials have low value commodities. Therefore, the transporting of the aggregate for a long distance to the operation location can considerably increase the price of the aggregate [50, 51, 52]. The closer aggregate sources are to the main roads the better, as this offers rapid and easy access to the road network for the delivery of aggregate Thus, to minimize the cost of transportation it is preferable during any construction project and cities or market centers to choose supplies of an aggregate quarry located near to those areas [53, 54; 55, 56], as well as reducing the costs for construction and maintenance of the roads to the quarries. The locations of the determined quarries were pinned and organized in Google Earth Pro. To estimate the distances between the quarries to the main roads, Google Earth Pro offers a feature (add path), to measure the length of a path and distance from these quarries to the main roads network in each region directly from the satellite images. Most of the quarries are located close to road networks, except for remote areas like the desert. The shortest distance to the road network indicates the suitability of a quarry's location as an aggregate resource [54]. Generally, the distance between quarries and the road network in all regions is less than 10 km, except for one quarry in the central region, which is 15 km from the road network. Figure 6 shows the distances between the quarries and the main road networks in all regions. In the northwest region, the distance ranges between 1 to 3 km except for the Vyadoket Croatian quarry, which is 8 km from the road network. In the central region, the distance ranges from 0.5 to 6 km, except for the Ostai quarry, which is 15 km from the road network. In the northeast region, the average distance ranges from 0.5 to 7 km. In the southwest region, the distance ranges from 0.6 to 2 km, except for the Al Amal Tareq quarry that is 7.5 km from the closest road alignment referred to as the road network. Therefore, the closest quarry to access to the road and to the main city has a high priority to use as an aggregate supplier to those locations, while the farthest quarry represents the low chance to use as an aggregate supplier.

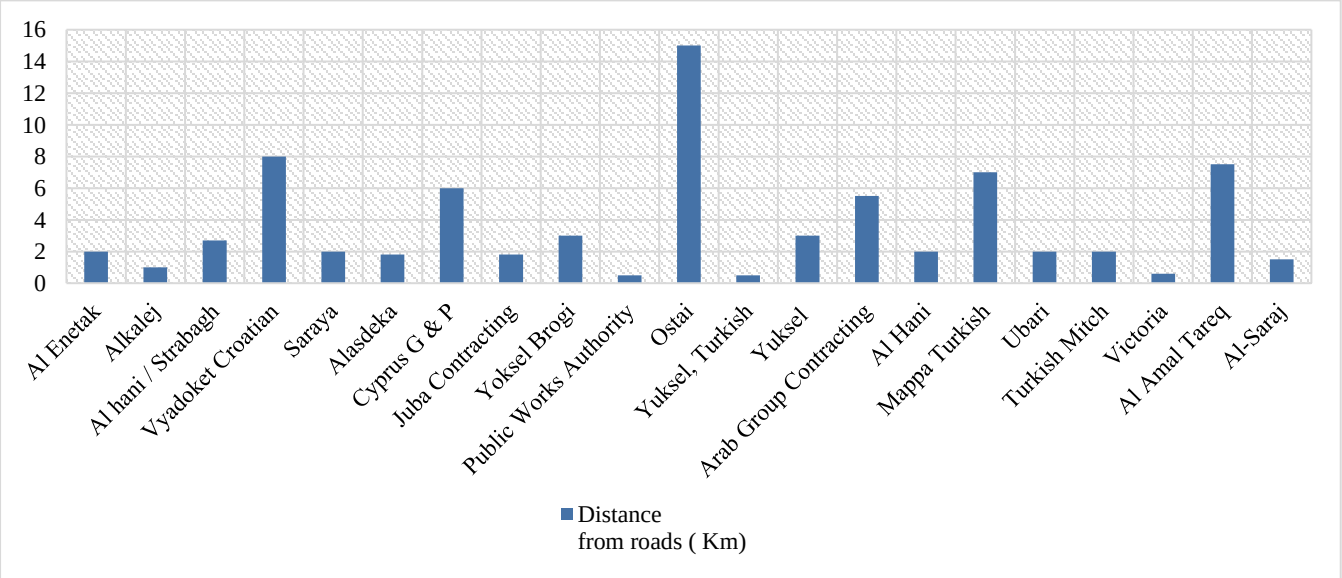

Figure 6: The distances between the quarries and the main road networks in all regions.

Results & Discussion

This paper estimates the potential inventory of aggregate sources on a country scale for the state of Libya. The total potential aggregate is 38.3 million tons. Figure 7 shows the spatial estimated aggregate amounts of Libya State. The circle size indicates the amount of potential aggregates at each site.

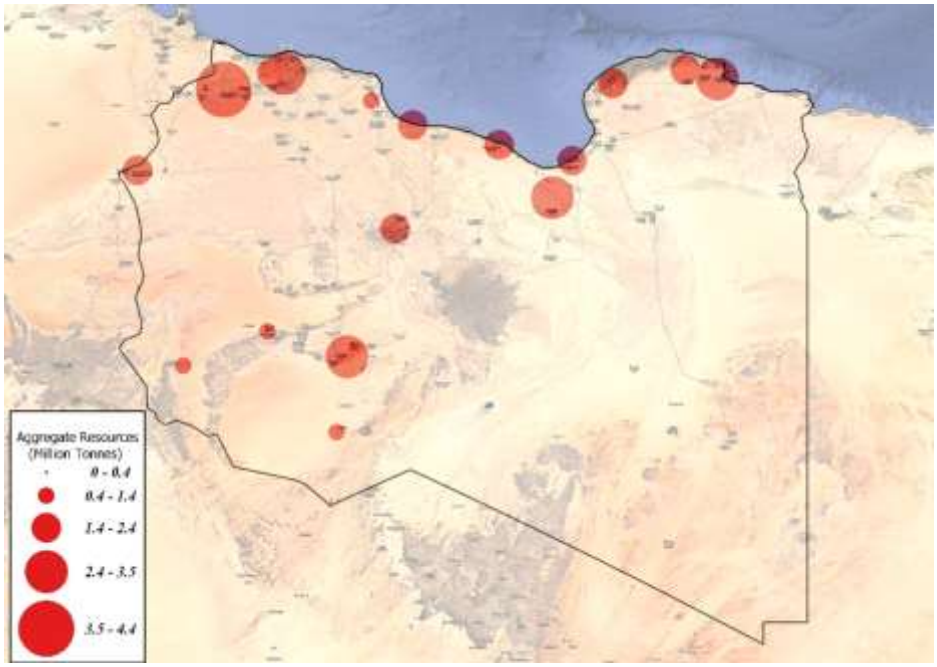

Figure 7: The spatial estimated aggregate amounts of Libya State.

The largest potential sources of aggregate are in quarries in the northwest region, with approximately 12 million tons of potential aggregate material available for extraction, as shown in graph 1. That 12 million tons represents thirty-one percent of the total potential aggregates in the country. The lowest potential sources of aggregate are in the southwest region with 5 million tons, representing thirteen percent of the total. The central region has 11.1 million tons of potential aggregate, which represents twenty-nine percent of the total potential aggregate, and the northeast region has 10.1 million tons. Limestone and dolomite are the predominant rock types in all the regions' quarries, except in the southwest region where sandstone is the main rock type. Figure 8 shows the percentage quantity of aggregate in each region.

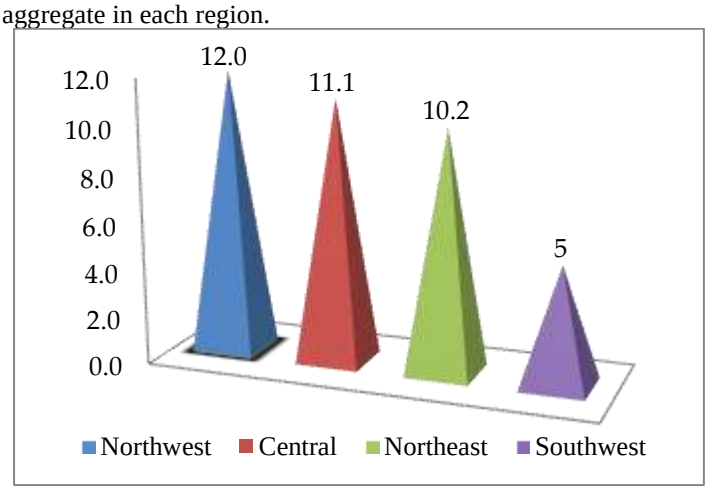

Figure 8: The quantity of aggregate by region.

The average distance from the quarry to the main road in all the regions' quarries is 3.6 km. However, seventy-one percent of the aggregate quarries are sited within 5 km of the main road. Overall, the northwest region's quarries have the highest inventory of aggregate, and they have the most suitable access to the road network compared to the other regions as shown in Figure 9.

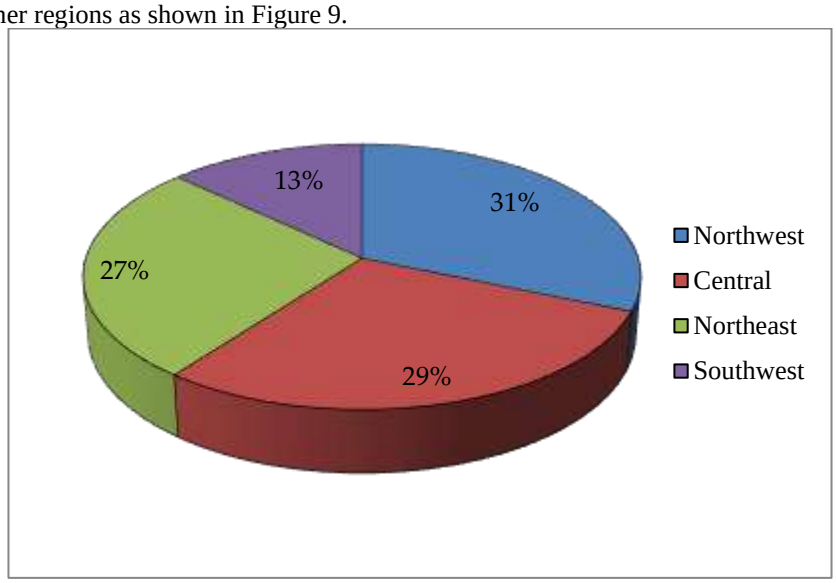

Figure 9: The percentage quantity of aggregate in each region.

Conclusion

This paper presents a reliable and repeatable technique to estimate and determine the potential inventory of aggregate sources on a country scale using Google Earth Pro® software and available national data publications. A case study state of Libya. During the shortage of information, we believe that the Google Earth Pro® method can provide reliable data for the aggregate inventory.

There are 21 operating quarries used as a source of aggregate for road construction. The main quarry locations are divided into four main geographic zones. The total potential aggregate is 38.3 million tons. The largest potential sources of aggregate are in quarries in the northwest region. The lowest potential sources of aggregate are in the southwest region. The average distance from the quarry to the main road in all the regions' quarries is 3.6 km. However, seventy-one percent of the aggregate quarries are sited within 5 km of the main road. Overall, the northwest region's quarries have the highest inventory of aggregate, and they have the most suitable access to the road network compared to the other regions.

The availability and accessibility of resources for gathering relevant information on road construction materials are limited in many developing countries. This work provides an overview of the potential inventory of aggregate sources for road construction in a country; however, detailed fieldwork and extensive geotechnical tests of appropriate geological formations are still required to determine a detailed potential aggregate inventory. Since this method relies on free published satellite images. This method should be repeatable every few years to measure and track the changes in the inventory. so long as adequate, Google Earth Pro® high-resolution aerial images are available. The ongoing demand for road construction will be depleting the inventory of natural materials. Developing policies to manage and control the use of basic materials to meet current and future needs is, therefore, a high priority for efficient and careful planning.

- Suggestions for future research Google Earth Pro® is a free and reliable technique and can be used for future studies.
- This technique should be repeatable every few years to measure and track the changes in the inventory.
- Incorporate other methods if possible, such as detailed fieldwork and extensive geotechnical tests of appropriate geological formations to additional calibration of the Google Earth pro estimations.
- Conduct aggregate inventories in other developing countries using the same technique.

References

[1]. Ness, D. (2008). Sustainable urban infrastructure in China: Towards a Factor 10 improvement in resource productivity through integrated infrastructure systems. *The International Journal of Sustainable Development & World Ecology*, *15*(4), 288-301.

[2]. Junior, P., & Franks, D. M. (2022). Construction materials and sustainable development. In *Routledge Handbook of the Extractive Industries and Sustainable Development* (pp. 228-246): Routledge.

[3]. Langer, W. H., & Ellefsen, K. J. (2001). *Natural Aggregate—Geophysical Opportunities.* Paper presented at the Symposium on the Application of Geophysics to Engineering and Environmental Problems 2001.

[4]. Langer, W. H., & Glanzman, V. (1993). *Natural aggregate, building America's future* (2330-5703).

[5]. Tepordei, V. (2001). US aggregates industry—an overview. *Aggreg. Magag*, *5*(11), 13-15.

[6]. Fischer, J. M., & Amekudzi, A. (2011). Quality of life, sustainable civil infrastructure, and sustainable development: Strategically expanding choice. *Journal of urban planning and development*, *137*(1), 39-48.

[7]. Luttig, G. (1994). *Rational management of the geo-environment.* Paper presented at the Aggregates-Raw Malerials' Giant Report on the 2n" International Aggregate Symposium.

[8]. Torres, A., Simoni, M. U., Keiding, J. K., Müller, D. B., zu Ermgassen, S. O., Liu, J., ... & Lambin, E. F. (2021). Sustainability of the global sand system in the Anthropocene. *One Earth*, *4*(5), 639-650.

[9]. Bisht, A. (2021). Conceptualizing sand extractivism: Deconstructing an emerging resource frontier. *The Extractive Industries and Society*, *8*(2), 100904.

[10]. Abdulrasool, A. T., Mohammed, S. S., Kadhim, N. R., & Hussain, W. A. M. (2022). *Sustainable Materials Used as Lightweight Aggregate:(An Overview).* Paper presented at the IOP Conference Series: Earth and Environmental Science.

[11]. Blengini, G. A., Garbarino, E., Šolar, S., Shields, D. J., Hámor, T., Vinai, R., & Agioutantis, Z. (2012). Life Cycle Assessment guidelines for the sustainable production and recycling of aggregates: the Sustainable Aggregates Resource Management project (SARMa). *Journal of Cleaner Production*, *27*, 177-181.

[12]. Barakat, A., Ouargaf, Z., & Touhami, F. (2016). Identification of potential areas hosting aggregate resources using GIS method: a case study of Tadla-Azilal Region, Morocco. *Environmental Earth Sciences*, *75*(9), 774. doi:10.1007/s12665-016-5613-6

[13]. Premasiri, H. R., & Dahanayake, T. (2018). *Development of GIS based model for locating sustainable construction aggregate mining sites: Case study from Sri Lanka.* Paper presented at the Proceedings of the Asian Conference on Remote Sensing.

[14]. Ojo, S. A., Olusina, J. O., Ngene, B. U., Busari, A. A., Adediran, J., & Eletu, A. (2019, November). Assessment of road infrastructure using remote sensing and GIS methodology for monitoring the condition of paved and unpaved roads. In *IOP Conference Series: Materials Science and Engineering* (Vol. 640, No. 1, p. 012099). IOP Publishing.

[15]. Bendixen, M., Iversen, L. L., Best, J., Franks, D. M., Hackney, C. R., Latrubesse, E. M., & Tusting, L. S. (2021). Sand, gravel, and UN Sustainable Development Goals: Conflicts, synergies, and pathways forward. *One Earth*, *4*(8), 1095-1111.

[16]. Wilson, D., Kieu, M., Sheng, M. S., Sreenivasan, A., Ivory, V., & Sharp, B. (2022). A Review of Aggregates for Land Transport Infrastructure in New Zealand. *Transportation Infrastructure Geotechnology*, 1-22.

[17]. Wu, M., Jin, H., Tang, B., Yang, L., Yang, T., & Gong, J. (2019, October). Constructing Topological Road Network of Wild Environment using Google Earth Pro. In *2019 IEEE Intelligent Transportation Systems Conference (ITSC)* (pp. 2095-2100). IEEE.

[18]. Derrow-Pinion, A., She, J., Wong, D., Lange, O., Hester, T., Perez, L., ... & Velickovic, P. (2021, October). Eta prediction with graph neural networks in google maps. In *Proceedings of the 30th ACM International Conference on Information & Knowledge Management* (pp. 3767-3776).

[19]. Arzaa, M., Gila, M., Ortiz, J., & Martínez, S. Virtual Globes for UAV-based data integration: Sputnik GIS and Google Earth™ applications.

[20]. Okolie, C. J., Onyegbula, J. C., Arungwa, I. D., Ayoade, O. Q., Daramola, O. E., Orji, M. J., . . . Uyo, I. I. (2022). Positional Accuracy Assessment of Historical Google Earth Imagery. *arXiv preprint arXiv:2205.01969*.

[21]. Tsangaratos, P., Ilia, I., Hong, H., Chen, W., & Xu, C. (2017). Applying Information Theory and GIS-based quantitative methods to produce landslide susceptibility maps in Nancheng County, China. *Landslides*, *14*(3), 1091-1111.

[22]. Kuffer, M., Pfeffer, K., & Sliuzas, R. (2016). Slums from space—15 years of slum mapping using remote sensing. *Remote Sensing*, *8*(6), 455.

[23]. Avtar, R., Aggarwal, R., Kharrazi, A., Kumar, P., & Kurniawan, T. A. (2020). Utilizing geospatial information to implement SDGs and monitor their Progress. *Environmental monitoring and assessment*, *192*(1), 1-21.

[24]. Brilli, M., Giustini, F., Conte, A. M., Mercadal, P. L., Quarta, G., Plumed, H. R., ... & Belardi, G. (2015). Petrography, geochemistry, and cathodoluminescence of ancient white marble from quarries in the southern Phrygia and northern Caria regions of Turkey: Considerations on provenance discrimination. *Journal of Archaeological Science: Reports*, *4*, 124-142.

[25]. Liew, T.-S., Price, L., & Clements, G. R. (2016). Using Google Earth to improve the management of threatened limestone karst ecosystems in Peninsular Malaysia. *Tropical Conservation Science*, *9*(2), 903-920.

[26]. Török, Á., Bögöly, G., Somogyi, Á., & Lovas, T. (2020). Application of UAV in topographic modelling and structural geological mapping of quarries and their surroundings—delineation of fault-bordered raw material reserves. *Sensors*, *20*(2), 489.

[27]. Labzovskii, L. D., Belikov, D. A., & Damiani, A. (2022). Spaceborne NO2 observations are sensitive to coal mining and processing in the largest coal basin of Russia. *Scientific Reports*, *12*(1), 1-11.

[28]. Ashtiani, M. Z., Muench, S. T., Gent, D., & Uhlmeyer, J. S. (2019). Application of satellite imagery in estimating stockpiled reclaimed asphalt pavement (RAP) inventory: a Washington State case study. *Construction and building materials*, *217*, 292-300.

[29]. Kulawiak, M., Dawidowicz, A., & Pacholczyk, M. E. (2019). Analysis of server-side and client-side Web-GIS data processing methods on the example of JTS and JSTS using open data from OSM and geoportal. *Computers & Geosciences*, *129*, 26-37.

[30]. Yang, L., Driscol, J., Sarigai, S., Wu, Q., Chen, H., & Lippitt, C. D. (2022). Google earth engine and artificial intelligence (ai): a comprehensive review. *Remote Sensing*, *14*(14), 3253.

[31]. Bakiyev, M., & Khasanov, K. (2019). DEFINITION OF THE VOLUME OF QUARRIES ON THE RIVERBED AT MINING OF ALLUVIAL SAND AND GRAVEL MATERIALS BY USING REMOTE SENSING DATA. *Irrigation and Melioration*, *3*(17), 4.

[32]. Gahlot, N., Prusty, G., & Dhara, M. (2022). Potential of Multi-resolution Satellite Imagery Products for Scale Variant Topographic Mapping. *Journal of the Indian Society of Remote Sensing*, *50*(1), 175-187.

[33]. Jayawardena, C., Thiruchittampalam, S., Dassanayake, A., Abeysinghe, A., & Wimalarathna, W. (2018). *A Proximity Based Rehabilitation Approach for Abandoned Quarries in Rural Sri Lanka.* Paper presented at the 2018 Moratuwa Engineering Research Conference (MERCon).

[34]. Garba, H. A., Ojeh, V. N., Elijah, E., & Ayeni, B. E. (2018). The Use of GIS and Google Earth Images for Mapping of Taraba State University Campus. *Asian Journal of Geographical Research*, 1-16.

[35]. Nuswanti, D. A., Mahendra, M. Z., & Aghastya, A. (2020). *Planning Reactivation Train for Kedungjati–Tuntang Using Google Earth, Global Mapper, and AutoCAD Civil 3D.* Paper presented at the 2nd International Symposium on Transportation Studies in Developing Countries (ISTSDC 2019).

[36]. Khoderchah, E., Jazzar, I., El-Zahab, S., Semaan, N., & Al-Sakkaf, A. (2020, November). Traffic-Lights-Based Guidance System in Lebanon using Network Optimization. In *2020 International Conference on Decision Aid Sciences and Application (DASA)* (pp. 331-334). IEEE.

[37]. Li, Q., Guo, H., Luo, L., & Wang, X. (2022). Automatic Mapping of Karez in Turpan Basin Based on Google Earth Images and the YOLOv5 Model. *Remote Sensing*, *14*(14), 3318.

[38]. Li, D., & Lu, M. (2018). Integrating geometric models, site images and GIS based on Google Earth and Keyhole Markup Language. *Automation in Construction*, *89*, 317-331.

[39]. Ashtiani, M. Z., & Muench, S. T. (2022). Using construction data and whole life cycle assessment to establish sustainable roadway performance benchmarks. *Journal of Cleaner Production*, 135031.

[40]. Smith, J. Promoting Sustainability in Infrastructure Through Quantifying Reclaimed Asphalt Pavement–An Ontario Municipal Case Study. *"Innovation in Pavement Management, Engineering and Technologies*" Session of the 2019 Conference of the Transportation Association of Canada Halifax, NS.

[41]. Cass, D., & Mukherjee, A. (2011). Calculation of greenhouse gas emissions for highway construction operations by using a hybrid life-cycle assessment approach: case study for pavement operations. *Journal of Construction Engineering and Management*, *137*(11), 1015-1025.

[42]. Choi, K., Lim, W., Chang, B., Jeong, J., Kim, I., Park, C. R., & Ko, D. W. (2022). An automatic approach for tree species detection and profile estimation of urban street trees using deep learning and Google street view images. *ISPRS Journal of Photogrammetry and Remote Sensing*, *190*, 165-180.

[43]. Ning, H., Li, Z., Ye, X., Wang, S., Wang, W., & Huang, X. (2022). Exploring the vertical dimension of street view image based on deep learning: a case study on lowest floor elevation estimation. *International Journal of Geographical Information Science*, *36*(7), 1317-1342.

[44]. Yang, X., Jiang, G. M., Luo, X., & Zheng, Z. (2012). Preliminary mapping of high-resolution rural population distribution based on imagery from Google Earth: A case study in the Lake Tai basin, eastern China. *Applied Geography*, *32*(2), 221-227.

[45]. Lee, R. L., Wong, G. M., Wong, S. Y., & Koh, A. C. (2020). Use of Singapore's "Standard Details of Road Elements" for distance estimation in traffic crash reconstruction: a comparison with onsite measurements and Google Earth Pro. *Forensic science international*, *313*, 110260.

[46]. Lin, L., Hao, Z., Post, C. J., Mikhailova, E. A., Yu, K., Yang, L., & Liu, J. (2020). Monitoring land cover change on a rapidly urbanizing island using Google Earth Engine. *Applied Sciences*, *10*(20), 7336.

[47]. Ashtiani, M. Z., Muench, S. T., Gent, D., & Uhlmeyer, J. S. (2019). Application of satellite imagery in estimating stockpiled reclaimed asphalt pavement (RAP) inventory: a Washington State case study. *Construction and Building Materials*, *217*, 292-300.

[48]. Rowell, D. (2010). 28. Project Unit 10-021. Aggregate Resources Inventory of the County of Simcoe, Southern Ontario.

[49]. Idris, F. (2012). *A study to document the properties of the aggregates used in the implementation of asphalt mixtures in various regions of Libya (in Arabic).* (Master). University of Tripoli, Libya.

[50]. Leighton, M. (1991). *Industrial minerals resource identification and evaluation.* Paper presented at the Industrial Minerals of the Midcontinent–Proceedings of the Midcontinent Industrial Minerals Workshop: US Geological Survey Bulletin.

[51]. Ma, M., Tam, V. W., Le, K. N., & Osei-Kyei, R. (2022). Factors affecting the price of recycled concrete: A critical review. *Journal of Building Engineering*, *46*, 103743.

[52]. Zhang, Y., Luo, W., Wang, J., Wang, Y., Xu, Y., & Xiao, J. (2019). A review of life cycle assessment of recycled aggregate concrete. *Construction and Building Materials*, *209*, 115-125.

[53]. Karakaş, A. (2014). Defining the suitability of new crushed rock aggregate source areas in the North of Kocaeli Province using GIS. *Bulletin of Engineering Geology and the Environment*, *73*(4), 1183-1197. doi:10.1007/s10064-013-0557-5

[54]. Barakat, A., Ouargaf, Z., & Touhami, F. (2016). Identification of potential areas hosting aggregate resources using GIS method: a case study of Tadla-Azilal Region, Morocco. *Environmental Earth Sciences*, *75*(9), 1-16.

[55]. Silva, R. V., De Brito, J., & Dhir, R. K. (2019). Use of recycled aggregates arising from construction and demolition waste in new construction applications. *Journal of Cleaner Production*, *236*, 117629.

[56]. Hochstetter, F. T., Haoa, S. R., Lipo, C. P., & Hunt, T. L. (2011). A public database of archaeological resources on Easter Island (Rapa Nui) using Google Earth. *Latin American Antiquity*, 385-397.